Int. J. Electrochem. Sci., 10 **(2015)** 870 - 882

International Journal of
ELECTROCHEMICAL
SCIENCE
www.electrochemsci.org

Electrochemical Behavior of Smart N-Isopropyl Acrylamide Copolymer Nanogel on Steel for Corrosion Protection in Acidic Solution

Ayman M. Atta[1,2], *Gamal A. El-Mahdy*[1,3,*], *Hamad A. Al-Lohedan*[1] *and Kamel R. Shoueir*[4]

[1]Department of Chemistry, College of Science, King Saud University, Riyadh 11451, Kingdom of Saudi Arabia.
[2] Egyptian Petroleum Research Institute, 1 Ahmad Elzomor St., Nasr city,Cairo, Egypt.
[3] Chemistry Department, Faculty of Science, Helwan University, Helwan, Egypt.
[4]Chemistry Department, Faculty of Science, Mansoura University, Mansoura, Egypt
[*]E-mail: gamalmah2000@yahoo.com

Received: 25 September 2014 / *Accepted:* 12 November 2014 / *Published:* 2 December 2014

Nanostructured composites increase their sensitivity and performance when employed as material in corrosive environments. In the present study, poly(2-acrylamido-2-methyl-1-propane- sulfonic acid - co-N-isopropylacrylamide) hydrogels, were synthesized by free- radical crosslinking solution polymerization with different ratios of monomers to form colloidal hydrogels shell around poly(vinyl alcohol) core through epichlorohydrine, in order to obtain well-define PVA(AMPS-NIPAm) core/shell nanogels with diameter nearly 30nm, which characterized by Fourier transform infrared spectroscopy (FTIR), transmission electron microscopy (TEM) and dynamic light scattering (DLS) . The inhibition effect of PVA-NIPAm/AMPS nanogel on the corrosion of steel in 1.0 M HCl solution was studied by potentiodynamic polarization curves and electrochemical impedance spectroscopy (EIS). Potentiodynamic polarization studies indicate that the new PVA-NIPAm/AMPS nanogel is a mixed inhibitor. Impedance studies show that a protective film is formed on the steel surface in the presence of the inhibitor and exhibit its protective nature even at low concentration. The results of polarization measurements are in good agreement with those obtained from EIS data for acting PVA-NIPAm/AMPS nanogel as an efficient corrosion inhibitor in 1 M HCl.

Keywords: N-Isopropyl Acrylamide Copolymer Nanogel, Steel, Acid inhibition, Polarization, EIS

1. INTRODUCTION

The application of nanoparticles in the synthesis of anticorrosion materials is one of the most important accomplishments of nanotechnology. Application as a corrosion inhibitor is also used in the

synthesis of smart coatings. Because of their unique properties such as their lateral surfaces and high chemical reactivity, nanoparticles are able to carry a significant amount of corrosive inhibitor particles on their surfaces [1]. Polymer nanocomposites have attracted great research and development interests due to their wide applications in anticorrosion materials [1–3]. It is also reported that organic materials containing metal and metal oxide nanoparticles have better anticorrosion characteristics due to the formation of both uniform distribution and passive layers on the surface of metallic substrate [4-6]. Moreover, the use of nano- and microlayers as well as self-healing coatings as anticorrosion and antifouling was attracted great attention in the recent years [7-10]. Smart nanomaterials can be a novel solution to protect steel from corrosion, chemical damages or even environmental changes. The presence of materials in the nanoscale is a way of making it smart and provides enhancement in material life. This was referred to the ability of materials to cover all surfaces of the substrate even in the presence of cracks by capillary action [11].

Smart gels are usually prepared by the free radical polymerization of monomers in the presence of a di- or tri-functional crosslinking agent. They can be found either in bulk or in nano- or microparticles. The bulk smart gels are easy to handle, but have very slow response to environment, while the gel nanoparticles act quickly to an external stimulus [12]. The most common smart polymer is based on *N*-isopropylacrylamide (NIPAm) homopolymers, copolymers and grafts [13-16]. It is well established that the nanoparticles were linked together by covalent bonding; they cannot be re-dispersed into solution, in contrast to well-known colloidal aggregates [12]. In the present work, the application of dispersed nanogels based on NIPAm copolymer as anticorrosive layer to protect steel from corrosion in acidic medium is the main objective due to their ability to form self-assembled protective layer on steel [3]. The main idea of the present work is to synthesize a new class of nanogels to increase their dispersion in water. A new class of nanostructured polymer gels has been synthesized by crosslinking gel nanoparticles through covalent bonds between functional groups on the surfaces of neighboring particles in solutions. Thus, these gels have two levels of structural hierarchy: the primary network is crosslinked polymer chains in each individual particle, while the secondary network is a system of crosslinked nanoparticles. In this respect, we have designed covalent bonded disperse nanogel. Such nanostructured gels have new and unique properties than those conventional gels do not have, including a high surface area, a highly dispersed self-assemble nanogel at room temperature, and temperature-tunable heterogeneity on the nanometer scale. This work may lead to creating opportunities for technological applications in the fields of corrosion inhibition materials. The corrosion inhibition of the prepared nanogel in 1 M HCl will be investigated by different electrochemical techniques.

2. EXPERIMENTAL

2.1. Materials

N- Isopropylacrylamide (NIPAm, Across 99% purity) was re-crystallized from 1:5 (v:v) toluene and n-hexane mixture; 2-acrylamido-2-methyl-1-propane- sulfonic acid (AMPS), purchased from Acros; poly(vinyl alcohol) (PVA) (polymerization degree is 1750, purchased from Acros); N,N-methylene-bisacrylamide (MBA), epichlorohydrin (ECH; Fluka), ammonium peroxydisulfate (APS)

was used without further purification. , $Fe_2(SO_4)_3$ was purchased from (Merck & Co., Inc., Whitehouse Station, NJ, USA). Other reagents were grade and used as received. Materials Tests were performed on steel of the following composition (wt.%): 0.14% C, 0.57% Mn, 0.21% P, 0.15% S, 0.37% Si, 0.06% V, 0.03% Ni, 0.03% Cr and and the balance Fe. Prior to each experiment, the specimen was polished to mirror finish with (400, 600, 800, 1000 and 1600 and 2000) emery polishing papers, washed with distilled water, degreased with acetone and quickly immersed into the test solution after drying. The aggressive solutions of 1.0 M HCl were prepared by dilution of analytical grade 37% HCl with distilled water.

2.2. Preparation of nanogel

2.2.1. Synthesis of PVA nanoparticles:

PVA (2wt%) was dissolved in 100 mL of distilled water. A solution of 1.66 g NaOH in 3 mL of water was slowly added to adjust pH to 12 with vigorous stirring. Acetone (15 mL) was added to the PVA solution dropwise with stirring for 30 min. Then the solution was cooled at 10 ^{0}C for 24 h. The solution was turned to weak blue which indicated that the long chains of PVA collapsed to nanoparticles. The resulting nanoparticle dispersion was dialyzed five times.

2.2.2. Synthesis of NIPAm /AMPS nanoparticles:

The polymerization reaction was carried out in a 250 ml four-necked flask, 2.079 g (0.01 mol) of AMPS, 1.13 (0.1 mol) of NIPAm and 66 mg (6 mol %) of MBA were fully dissolved in 50 ml deionized water and then added dropwise to APS solution (0.5% in 50 mL deionized water) via the semi-batch method at intervals of 2h and reaction temperature of 70 ^{0} under nitrogen atmosphere. The Nanogel was separated from solution using ultracentrifuge at 22000 rpm three times.

2.2.3. Synthesis of PVA- NIPAm/AMPS nanogel:

PVA nanoparticle solution (1 g dispersed in 50 ml water) was mixed with both 1mL epichlorohydrin and NIPAm/AMPS) nanoparticle dispersed solution (1 g suspended in 50 mL water) and heated with stirring at 98 ^{0}C for 10 h under nitrogen atmosphere in order to obtain core/shell structure. The obtained dispersed nanogels could be frozen and lyophilized into freeze-dried powder PVA-NPAm/AMPS, which can be easily dispersed into water forming nanoparticle dispersion. The nanogel was also separated by precipitation into 10 folds of acetone and dispersed in water.

2.3. Characterization of PVA- NIPAm/AMPS nanogel:

Fourier transform infrared (FTIR) spectrometer (Nicolet, NEXUS-670) was used to elucidate the functional groups of the nanogels with a range 4000-400 cm^{-1} using KBr pellets.

TEM micrograph of colloidal nanogels particle were taken using a JEOL JEM-2100 electron microscope. A few drops of nanogel solution were diluted into 1 mL of ethanol, and the resulting ethanol solution was placed onto a carbon coated copper grid and allowed to evaporate. HR-TEM images of the nanocomposites were recorded using a JEM-2100F (JEOL) at an acceleration voltage of 200 kV.

Samples for dynamic light scattering (DLS) were prepared by diluting several drops of the nanogel solution into 2 mL of water under vigorous stirring. The DLS measurements were performed on a Brookhaven Instruments system (Santa Barbara, CA, USA) with a 514.5 nm argon ion laser (model 85 Lexel Laser) as the light source.

2.4. Electrochemical measurements:

Electrochemical experiments were carried out in the conventional three-electrode cell with a platinum counter electrode (CE), a saturated calomel electrode (SCE) and steel as working electrode (WE). All electrochemical measurements were carried out using a potentiostat (Solartron 1470E system) with Solartron 1455A as frequency response analyzer. Potentiodynamic polarization curves was scanned using a sweep rate of 1 mV/s. Electrochemical impedance spectroscopy (EIS) was carried out in the frequency range of 10 mHz–10 kHz. Polarization and Impedance data were analyzed using CorrView, Corr- Ware Zplot and ZView software, respectively.

3. RESULTS AND DISCUSSION

The nanoparticle networks can be made to retain some properties of their dispersions [17-20]. As a demonstration, we first made nanoparticles of copolymer N-isopropylacrylamide (NIPAm, molar fraction of 50%) and 2-acrylamido-2-methylpropane sulfonic acid (AMPS, 50%) using an free surfactant radical polymerization method [14]. The NIPAm has a thermally responsive property and provide its amide group for crosslinking sites, while the AMPS provides sulfonic groups (SO_3H) to form anionic gel in the presence of NaOH. The crosslinking polymer network was completed in the presence of MBA crosslinker as represented in the scheme 1. It was observed that upon exhaustive ultra-centrifugation, a concentrated NIPAm/AMPS nanoparticle dispersion was obtained with light blue color which can be referred to light interference from the closely packed nanoparticles. The glycidyl ether of PVA (EPVA) was obtained by reacting PVA with ECH as represented in the scheme 1. The presence of epichlorohydrin in the dispersion of EPVA and NIPAm/AMPS network (Scheme 1) was used to replace the water in the prepared nanoparticles. The crosslinking between epichlorohydrin and amide groups of NIPAm occurred and the nanoparticles formed a network after incubation at 98 ^oC for 10 h. The crosslinking could be ascribed to the inter-component reaction between amide of NIPAm and epoxide groups of EPVA, which was further evidenced by the reaction of model compounds [21]. This network was then transferred to acetone and finally to de-ionized water for thorough washing. In contrast to conventional gels, which are colorless, this nanoparticle network was

bright blue. A possible mechanism for the formation of networks is presented in the (Scheme 2). The primary network is composed of crosslinked polymer chains in each individual nanoparticle (EPVA or NIPAm/AMPS), while the secondary network is a system of crosslinked nanoparticles (PVA-NIPAm/AMPS).

3.1. Characterization of PVA-NIPAm/AMPS nanogel

FTIR spectrum of PVA-NIPAm/AMPS nanoparticle networks was represented in Figure 1. The presence of a sharp absorption band at 3392 cm^{-1} can be attributed the –OH stretching band of the PVA in the nanogels units or that produced from crosslinking between EPVA and NIPAm/AMPS networks (scheme 1c). The appearance of C-H stretching aliphatic at 2942 and 2870 cm^{-1} and disappearance of bands at 3000-3100 cm^{-1} indicates the complet polymerization of AMPS, NIPAm and MBA monomers. The primary amide carbonyl group bands of NIPAm units, and the secondary amide N-H deformation bands of AMPS units are observed at 1660 and 1550 cm^{-1} respectively. The bands at 1441 cm^{-1} indicates C-H bending of CH_2 groups and at 1328 cm^{-1} indicates the presence of the isopropyl group]. The band at 1143 cm^{-1}, and 1035 cm^{-1} indicates the presence of asymmetric and symmetric stretching of S-O bond of SO_3Na groups. The C-S stretching occurs at 621cm^{-1} which confirmed AMPS unit [22].

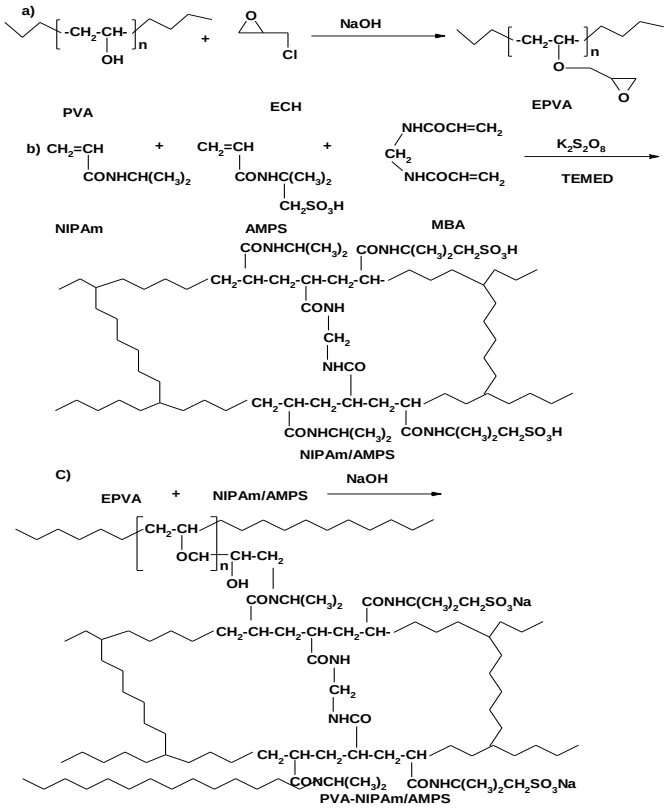

Scheme 1. Synthesis of a) EPVA, b)NIPAm/AMPS and c) PVA-NIPAm/AMPS nanogels.

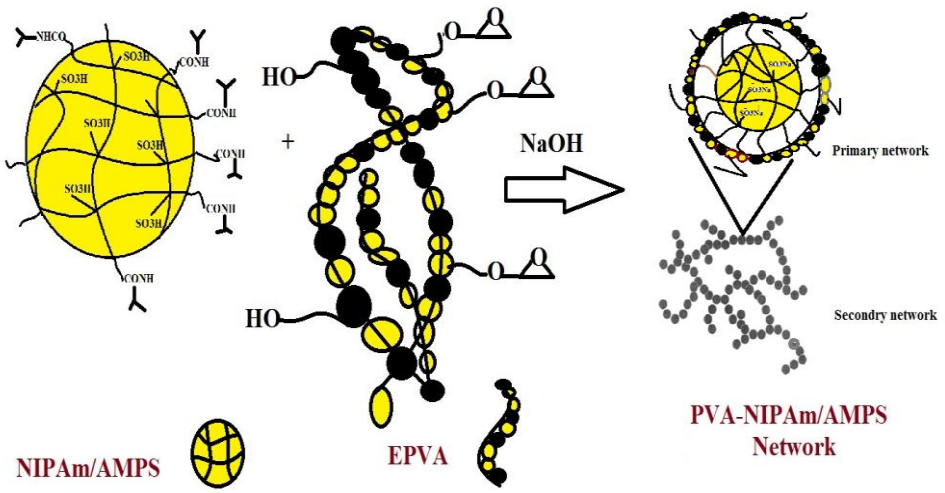

Scheme 2. Sketch of the gel PVA-NIPAm/AMPS nanoparticle networks.

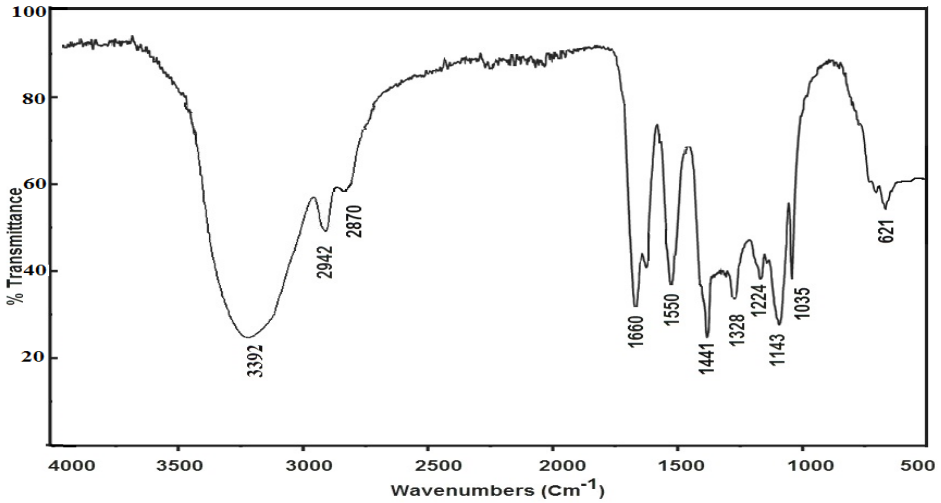

Figure 1. FTIR spectrum of PVA-NIPAm/AMPS nanogel.

The morphologies of the prepared networks can be analyzed from TEM micrographs Figure 2. Figure 1a shows that the EPVA polymer chains form aggregate about 150 nm in diameter and width. The PVA aggregates and they look like a spherical. Figure 2b shows the TEM micrograph of NIPAm/AMPS nanogel. In the previous work [23], we described the mechanism of the formation of NIPAm/AMPS network. In this respect, it can be expected that the size of NIPAm/AMPS nanogels, which contain high AMPS content, were larger than the NIPAm/AMPS nanogels contain low AMPS content. Figure 2b shows that, as expected NIPAm/AMPS nanogels appear dark or with partially transparent, non-uniform periphery which fades towards the boundary [23]. This was attributed to the higher crosslinked density and complex interlaced structure of NIPAm/AMPS networks. TEM analysis indicated that the average particle diameters ranged from 175 up to 200 nm. Figure 2c, PVA-NIPAm/AMPS, shows stabilized network as expected from scheme 2. It was noticed that the morphology was changed from spherical to particles constructed with a shell-like cactus or chestnut

shell. This may be attributed to strong hydrogen bonding between OH or glycidyl ether of EPVA inter-chains and NIPAm/AMPS networks. The size of PVA-NIPAm/AMPS particles was ranged from 150 to230 nm. It was also observed that, in addition to the almost perfectly round-shaped nanoparticles (Figure 2 b and c) there are an important number of defect structures (Figure 2c). This multitude of configurations may be understood in terms of the great ease of structural transformations during particle growth [24].

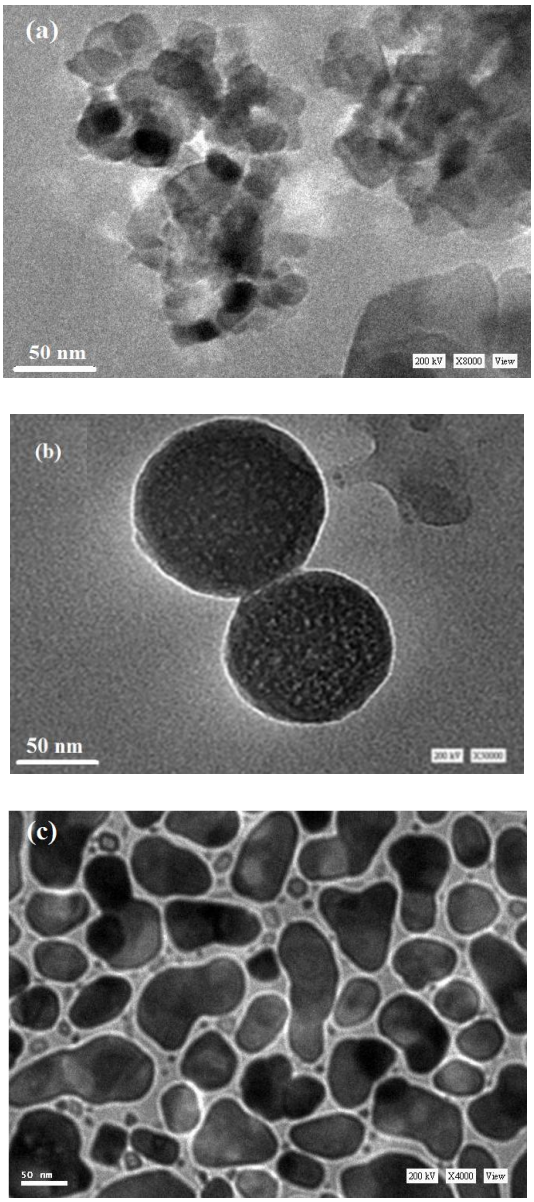

Figure 2. TEM micrographs of (a) EPVA, (b) NIPAm/AMPS and (c) PVA-NIPAm/AMPS nanogels.

The hydrodynamic diameter of PVA-NIPAm/AMPS nanogel was measured by dynamic light scattering (DLS). The corresponding DLS graph of PVA-NIPAm/AMPS nanogel was presented in Figure 3. DLS measurements of PVA-NIPAm/AMPS nanogel yielded a hydrodynamic average size of 143 nm. The data indicated the polydisperse nature of PVA-NIPAm/AMPS nanogel. DLS

measurements revealed that the PVA-NIPAm/AMPS nanogel molecules are highly dispersed in aqueous media. This colloid remains stable for three months without noticeable precipitation.

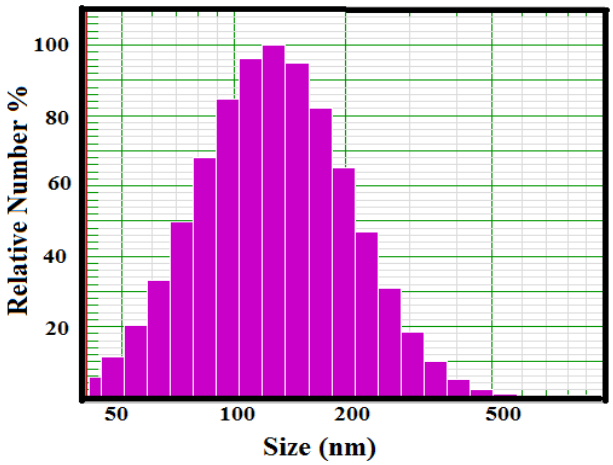

Figure 3. DLS data of PVA-NIPAm/AMPS nanogel

3.2. Polarization curves

Figure 4 shows the polarization curves for steel in 1 M HCl solution containing different concentrations of - PVA-NIPAm/AMPS nanogel. It can be seen from the polarization curves that in the presence of the PVA-NIPAm/AMPS nanogel there is a decrease in anodic and cathodic current densities, which shows the inhibitory effect of PVA-NIPAm/AMPS nanogel. This phenomenon occurs at all studied concentrations and indicated that - PVA-NIPAm/AMPS nanogel exhibits cathodic and anodic effects, Hence, PVA-NIPAm/AMPS nanogel can be classified as mixed type inhibitor in acid media. Electrochemical parameters, such as the anodic (ba) and cathodic (bc) Tafel slopes, corrosion potential (E_{corr}), corrosion current density (I_{corr}) are given in Table 1. It is clear that the corrosion current density (I_{corr}) decreased as the concentration of inhibitor increased. Polarization results show that the polarization resistance increase with the increasing PVA-NIPAm/AMPS nanogel concentration. Polarization data indicated that the adsorbed PVA-NIPAm/AMPS nanogel reduced the cathodic and anodic reactions, which were probably decreased by the surface blocking effect of the active sites on steel surface. Therefore, the inhibition effect of PVA-NIPAm/AMPS nanogel occurred by blocking the anodic sites on the steel surface thereby preventing anodic dissolution of the steel. This also caused a decrease in the surface area available for cathodic reaction. It can be observed that the values of corrosion current density (I_{corr}) of steel in the presence of the inhibitor were lower than that for the inhibitor free solution. This suggests that the compound was adsorbed on the steel surface and retarding the corrosion reactions. The decrease in I_{corr} can be attributed to the PVA-NIPAm/AMPS nanogel adsorption on the steel surface. These findings suggest that the inhibiting action of the inhibitor due to the adsorption of PVA-NIPAm/AMPS nanogel on steel surface and is highly influenced by the concentration of the inhibitor. The observed inhibition phenomenon is generally associated to the formation of a protective layer of adsorbed PVA-NIPAm/AMPS nanogel

on the steel surface [25]. The inhibition efficiency IE (%) was calculated using the following equation [26-28]:

$$\%IE = i_{corr} - i_{corr(inh)} / i_{corr} \quad (1)$$

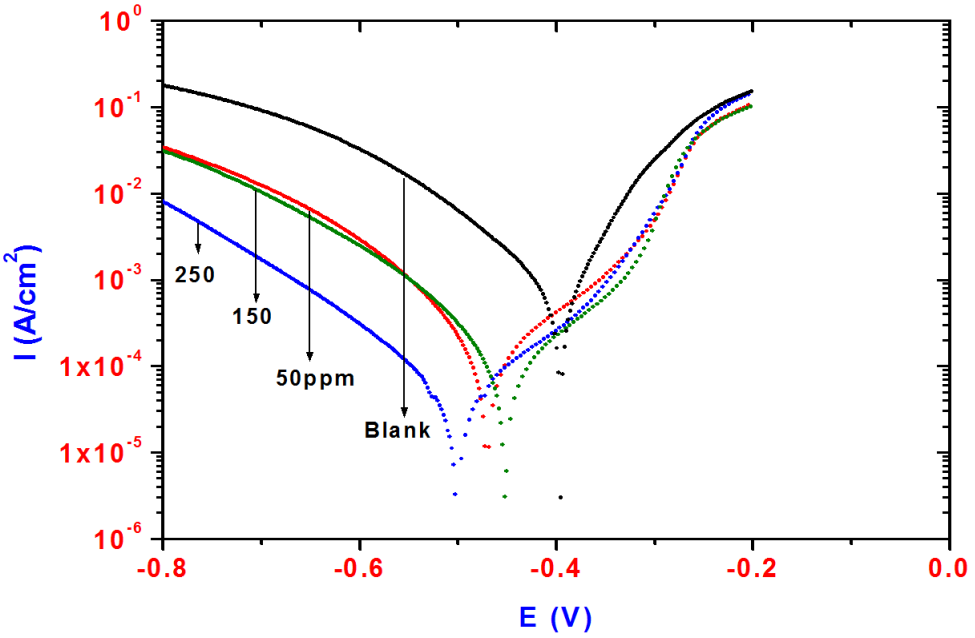

Figure 4. Polarization curves for steel in 1m HCl solution containing different concentrations of PVA-NIPAm/AMPS nanogel.

Table 1. Inhibition efficiency values for steel in 1M HCl with different concentrations of PVA-NIPAm/AMPS nanogel calculated by Polarization and EIS methods.

Polarization Method						EIS Method		
	Ba (mV)	Bc (mV)	E_{corr} (V)	i_{corr}, μA/cm^2	IE%	R_p, Ohm	Cdl (μF/cm^2)	IE%
Blank	69	120	-0.3955	839	____	1.80	334	____
50 ppm	138	98	-0.4703	151	82	35	130	82.8
150	110	95	-0.4515	87	89	19	112	90.5
250	134	124	-0.5007	50	94	10.5	106	94.8

where i_{corr} and $i_{corr(inh)}$ are the values of corrosion current density of uninhibited and inhibited specimens, respectively. The inhibition efficiency (IE%) calculated from the potentiodynamic polarization curves are presented in Table . The increase in inhibition efficiency observed at higher inhibitor concentrations indicates that more PVA-NIPAm/AMPS nanogel were adsorbed on the steel

surface, thus providing wider surface coverage and PVA-NIPAm/AMPS nanogel acted as adsorption inhibitors. Inhibition efficiency (IE) at 250 ppm reaches up to a maximum of 94 % , which confirms that PVA-NIPAm/AMPS nanogel is good inhibitor for steel in 1.0 M HCl.

3.3. Electrochemical impedance spectroscopy (EIS)

Figure 5 represents the Nyquist diagrams for steel in 1.0 M HCl in the presence of PVA-NIPAm/AMPS nanogel with different concentrations. All the impedance spectra exhibit one single capacitive loop, which indicates that the corrosion of steel is mainly controlled by the charge transfer process [29]. The diameter of the capacitive loop in the presence of inhibitor is larger than that in the absence of inhibitor (blank solution), and increases with the inhibitor concentration. All EIS spectra were analyzed using the equivalent circuit shown in Figure 6, which represents a single charge transfer reaction and fits well with our experimental results.

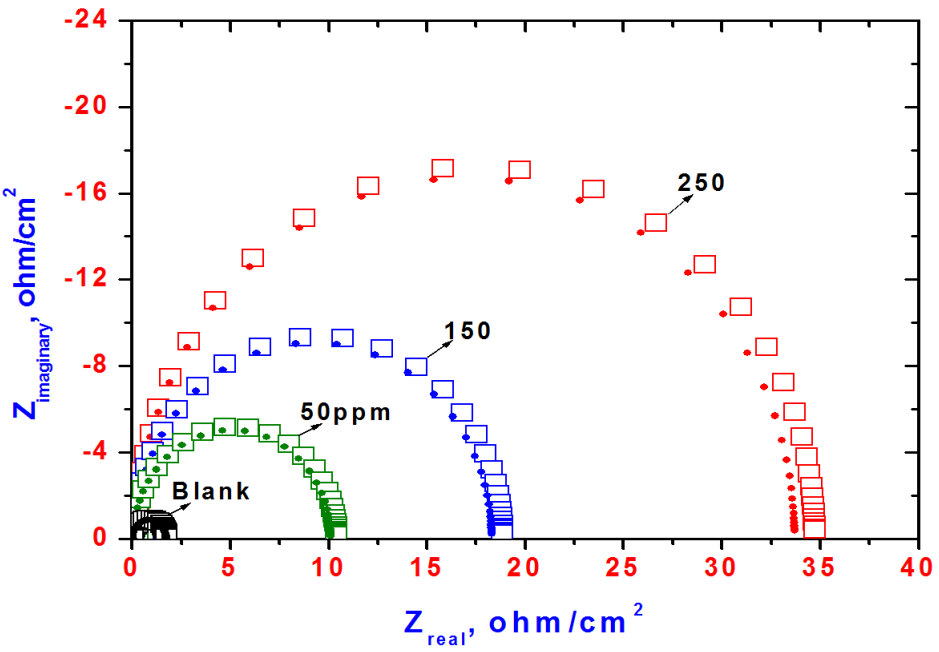

Figure 5. Nyquist plot for steel for steel in 1m HCl solution containing different concentrations of PVA-NIPAm/AMPS nanogel.

Rs represents the resistance of the solution and Rct represents the charge transfer resistance whose value is a measure of electron transfer across the surface and is inversely proportional to corrosion rate. The constant phase element, CPE, is introduced in the circuit instead of a pure double layer capacitor to give a more accurate fit [30]. The impedance of the CPE is expressed by the following expression:

$$Z_{CPE} = Y_0^{-1} (J\omega)^{-n}$$

where Y_0 is a proportional factor, $j^2 = -1$ is an imaginary number, and ω is the angular frequency ($\omega = 2\pi f$) . If n = 1, the impedance of CPE is identical to that of a capacitor, and in this case Y_0 gives a pure capacitance (C). Depending on the value of n, CPE can represent a capacitance (Z_{CPE} = C, n = 1), a resistance (Z_{CPE} = R, n = 0), inductance (Z_{CPE} =L, n = -1) and a Warburg impedance (Z_{CPE} = W, n = 0.5). The impedance parameters, including Rct and Cdl, obtained from fitting the recorded EIS data using the equivalent circuit of Figure 6 are listed in Table1 It is clear that the Rct values increased and the Cdl values decreased with increasing inhibitor concentration.

These results may be attributable to the adsorption of the PVA-NIPAm/AMPS nanogel onto the steel/solution interface. Evidently, the addition of PVA-NIPAm/AMPS nanogel decreases Cdl value [31] and the decrease in Cdl value was more pronounced at 250ppm. The double layer between the charged electrode surface and the solution is considered as an electrical capacitor. The adsorption of PVA-NIPAm/AMPS nanogel on the surface of steel can influence its electrical capacity. This can be explained by the water molecules replacement with PVA-NIPAm/AMPS nanogel. A decrease in Cdl value in the presence of PVA-NIPAm/AMPS nanogel proves the formation of the protective layer on the steel surface [32].The inhibition efficiency values (IE%) were calculated from Rct data using the following equation:

$$IE\% = 1- R_{ct\,(1)}/ R_{ct(2)} \times 100 \qquad (2)$$

where $R_{ct\,(1)}$ and $R_{ct\,(2)}$ are the charge transfer resistances in the HCl solution in the absence and in the presence of the inhibitors, respectively. It is clear from Table 1 that addition of PVA-NIPAm/AMPS nanogel to HCl solution caused a significant increase in the IE% values, which increase with inhibitor concentration.

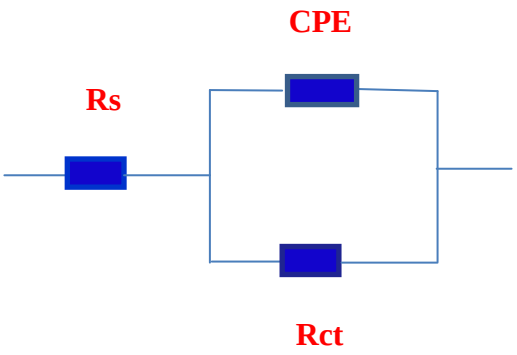

Figure 6. Equivalent circuit employed for fitting experimental data.

4. CONCLUSIONS

1.Electrochemical behavior of preformed smart N-Isopropyl acrylamide copolymer nanogel on steel for corrosion protection in acidic chloride solution is investigated using polarization and electrochemical impedance spectroscopy(EIS).

2. The electrochemical result shows that PVA-NIPAm/AMPS nanogel functioned as an efficient corrosion inhibitor for steel in 1 M HCl.

3. Polarization studies show a mixed-inhibition mechanism and its inhibition efficiency increased with the inhibitor concentration.

4. The electrochemical impedance data shows that the application of the PVA-NIPAm/AMPS nanogel significantly increased the Rct value and decreased the Cdl value in 1 M HCl, suggesting that corrosion inhibition on steel surface takes place by adsorption.

ACKNOWLEDGEMENT
This project was supported by King Saud University, Deanship of Scientific Research, College of Science Research Center.

References

1. M.Aliofkhazraei, Smart nanocoatings for corrosion detection and control, DOI: 10.1533/9780857096883.2.198, 2014 Woodhead Publishing Limited, 198-223.
2. M. Ionit, A. Pruna, *Prog. Org. Coat*.,72 (2011) 647.
3. A.M. Atta, O.E. El-Azabawy, H.S. Ismail, *Corros. sci.*, 53(2011) 1680.
4. A.M. Atta, G. A. El-Mahdy, H. A. Al-Lohedan, A. O. Ezzat, *Molecules* , *19*(2014) 10410.
5. A.M. Atta, G.A. El-Mahdy, H.A. Al-Lohedan, S. A. Al-Hussain, *Int. J. Mol. Sci. , 15*(2014), 6974.
6. G. A. El-Mahdy, A. M. Atta, H.A. Al-Lohedan, *J. Taiwan. Inst. Chem. E., 45 (2014)1947.*
7. T. T. Szabó, L. Románszki, M. Pávai. The use of nano-microlayers, self-healing and slow-release coatings to prevent corrosion and biofouling, *Handbook of Smart Coatings for Materials Protection, 2014, Pages 135-182,*
8. S. Hatami Boura, M. Peikari, A. Ashrafi, M. Samadzadeh, *Prog. Org. Coat., 75 (2012) 292.*
9. K.Zhang, L.Wang, W. Sun, G. Liu, *Corros. Sci., 88 (2014) 444.*
10. M.D. Hager, P. Greil, C. Leyens, S. van der Zwaag, U.S. Schubert, *Adv. Mater*., 22 (2010) 5424.
11. D.Y. Wu, S. Meure, D. Solomon, *J. Prog. Polym. Sci.* 33 (2008) 479.
12. Z. Hu, X. Lu, J. Gao, C. Wang, *Adv. Mater*., 12 (2000) 1173.
13. A. M. Atta, S. Abdel-Azim, A. Abdel-Azim, *J. Disper. Sci. Tecnol.*, 31(2010)1552.
14. A. M. Atta, A. K. F. Dyaba, H. A. Allohedan, *Polym. Advan. tech.*, 24 (2013) 986.
15. A. M. Atta, N.E. Maysour, *J. Polym. Res.*, 13 (2006) 53.
16. M. A. Akl, A.A. Sarhan, K. R. Shoueir, A.M. Atta, *J. Disper. Sci. Tecnol.*, 34 (2013)1399.
17. R. H. Pelton, P. Chibante, *Colloid. Surf.*, 20 (1986) 247.
18. S. Hirotsu, Y. Hirokawa, T. Tanaka, *J. Chem. Phys*., 87 (1987) 1392.
19. Y. Li, G. Wang, Z. Hu, *Macromolecules*, 28 (1995) 4194.
20. E. A. Kamenetzky, L. G. Magliocco, H. P. Panzer, *Science*, 263 (1994) 207.
21. J. Mu, S. Zheng, *J. Colloid. Interf. Sci*., 307 (2007) 377.
22. C. Zhang, A.J. Easteal, *J. Appl. Polym. Sci.*, 104 (2007) 1723.
23. A. M. Atta, H. Al-Shafey, *Int. J. Electrochem. Sci.*, 8 (2013) 4970.
24. S. Iijima, *J Electron. Microsc.*, 34 (1985)249.
25. X.H. Li, S.D. Deng, H. Fu, T.H. Li, *Electrochim. Acta* 54 (2009) 4089.
26. Q. Qu, Z. Hao, L. Li, W. Bai, Z. Ding, *Corros. Sci.* 51 (2009) 569.
27. F. Bentiss, M. Lebrini, M. Lagrenée, *Corros. Sci*. 47 (2005) 2915.
28. Q. Qu, S. Jiang, W. Bai, L. Li, *Electrochim. Acta* 52 (2007) 6811.
29. M. Behpour, S.M. Ghoreishi, N. Mohammadi, N. Soltani, M. Salavati-Niasari, *Corros. Sci*. 52 (2010) 4046.

30. M. Behpour, S.M. Ghroreishi, N. Soltani, M. Salavati-Niasari, M. Hamadanian, A.
31. Gandomi, *Corros. Sci*. 50 (2008) 2172.
32. R. Fuchs-Godec, M.G. Pavlovic, *Corros. Sci*. 58 (2012) 192.
33. N.S. Patel, S. Jauhari, G.N. *Mehta, Acta Chim. Slov*. 57 (2010) 297.